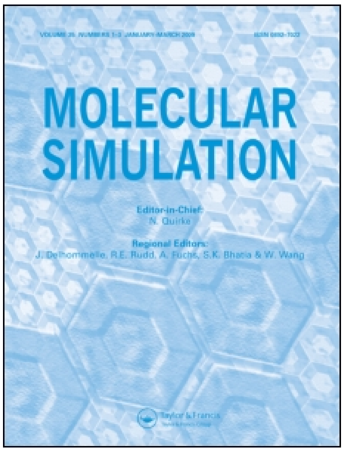

**Molecular Simulation**
Publication details, including instructions for authors and subscription information:
http://www.informaworld.com/smpp/title~content=t713644482

# Molecular Simulation of Adsorption Processes. 1. Isothermal Stirred-tank Adsorber

J. P. B. Mota[a]; I. A. A. C. Esteves[a]
[a] Departamento de Química, Centro de Química Fina e Biotecnologia, Faculdade de Ciências e Tecnologia, Universidade Nova de Lisboa, Caparica, Portugal

**To cite this Article** Mota, J. P. B. and Esteves, I. A. A. C.(2004) 'Molecular Simulation of Adsorption Processes. 1. Isothermal Stirred-tank Adsorber', Molecular Simulation, 30: 6, 387 — 396

**To link to this Article: DOI:** 10.1080/08927020310001659944

**URL:** http://dx.doi.org/10.1080/08927020310001659944

*Molecular Simulation*, Vol. 30 (6), 15 May 2004, pp. 387–396

# Molecular Simulation of Adsorption Processes. 1. Isothermal Stirred-tank Adsorber

J.P.B. MOTA* and I.A.A.C. ESTEVES

*Departamento de Química, Centro de Química Fina e Biotecnologia, Faculdade de Ciências e Tecnologia, Universidade Nova de Lisboa, 2829-516 Caparica, Portugal*

*(Received April 2003; In final form November 2003)*

**A new molecular simulation method is proposed to solve the governing equations for a multicomponent, isothermal stirred-tank adsorber under equilibrium controlled conditions. The technique is formulated in the Gibbs ensemble, but is more appropriately viewed as a hybrid of a molecular simulation and continuum modeling. For the general case of an arbitrary multicomponent mixture, the total number of molecules of each species is allowed to fluctuate so that the ensemble average satisfies the macroscopic material balances to the adsorber. It is shown that if an analytical equation of state for the fluid phase is known, the simulation procedure can be considerably simplified and acquires many characteristics of a Monte Carlo simulation conducted in the grand canonical ensemble. The technique is thoroughly validated and its usefulness is demonstrated through application to a gas separation problem encompassing the major steps of practical value to batch adsorption processes.**

*Keywords*: Adsorption of fluids and fluid mixtures; Molecular simulation method; Isothermal stirred-tank adsorber; Grand Canonical Monte Carlo (GCMC) method

## INTRODUCTION

The adsorption of fluids and fluid mixtures is a research field in which theory and computer simulation have contributed greatly to our understanding of the phenomena involved [1]. It is therefore not surprising that computational modeling has been a key enabling tool in adsorption technology for process development and design, equipment sizing and rating, and process optimization.

Traditionally, the behavior of the separation unit to a given set of input parameters and operating conditions has been evaluated by application of an engineering model. However, the success of the model is critically dependent upon accurate knowledge of thermodynamic properties and phase equilibrium behavior. Thanks to advances made over the past decade, molecular simulation has developed to the point where it is now useful for quantitative prediction of those properties, and can circumvent some of the limitations of traditional thermodynamic models [2]. But despite the general awareness of the potential applications of molecular modeling, its integration into process design still remains largely unexplored.

The principal molecular method that has been used to study adsorption is the Grand Canonical Monte Carlo (GCMC) method [3] (one of the earliest GCMC studies of adsorption dates back to 1982 [4]). The chemical potential of the components in the system (as well as the volume and temperature) is specified in advance and the equilibrium number of adsorbed particles is calculated as an ensemble average. However, in process modeling one is often interested in other views of the phase behavior, beyond that of the traditional adsorption isotherm provided by the GCMC method. The first breakthrough in molecular simulation of phase equilibria was the invention of the Gibbs Ensemble Monte Carlo (GEMC) method [5–7], which gives the same type of phase coexistence information obtained from a flash calculation. The method has been used, for example, to determine capillary condensation [8,9] and liquid–liquid phase diagrams [10] in confined systems. More recently, Gibbs-Duhem Integration (GDI) techniques [11,12], semigrand ensemble [13,14] and pseudoensemble Monte Carlo methods [15–18] have been developed to trace several types

---

*Corresponding author. Tel.: +351-212948300. Fax: +351-212948385. E-mail: pmota@dq.fct.unl.pt

ISSN 0892-7022 print/ISSN 1029-0435 online © 2004 Taylor & Francis Ltd
DOI: 10.1080/08927020310001659944

of phase diagrams. Unfortunately, the application of these techniques in adsorption studies is still scarce.

Here, we propose a new molecular simulation method that, in a certain sense, provides a direct bridge between disparate spatial scales—molecular and macroscopic—and apply it to solve the conservation equations for a multicomponent batch adsorber. This process unit is of fundamental importance in adsorption technology, because despite its simplicity it encompasses the major features of more complex adsorption units. In fact, it can be regarded as the basis for all other adsorption separation processes. The method, as presented here, is currently limited to an isothermal unit under equilibrium-controlled conditions.

Our approach employs a basic idea behind the GDI and pseudoensemble Monte Carlo methods: a macroscopic model is established based on differential material balances to the separation unit and a series of molecular simulations is conducted that integrate along the path described by the model. Special care is taken in the formulation of the method so that the integration is accomplished without the need for fluctuation quantities, since these are measured less precisely than simple ensemble averages. The method is thoroughly validated through a series of tests in which the results are checked against GCMC simulations. The usefulness of the method is demonstrated through simulation of a typical operation of the batch adsorption unit. Some concluding remarks are provided at the end.

## PROBLEM FORMULATION

We begin by establishing the model for an isothermal stirred-tank adsorber under equilibrium-controlled conditions. The system under consideration is sketched in Fig. 1. The following notation is adopted: $\eta$ is the bulk porosity (volumetric fraction of the adsorber which is filled with fluid phase), $\eta_{\mathrm{P}}$ is the internal porosity of the adsorbent, $F_i \geq 0$ is the amount of component $i$ added to the adsorber in the inlet stream, and $W_i \geq 0$ is the corresponding amount removed in the outlet stream; both $F_i$ and $W_i$ are defined per unit volume of adsorber.

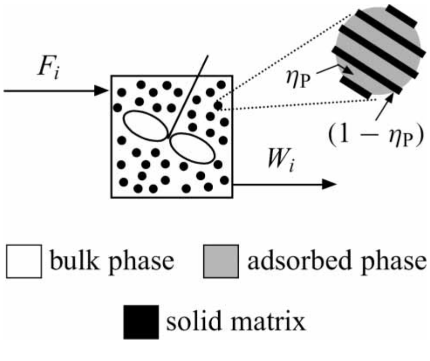

FIGURE 1 Schematic representation of an isothermal stirred-tank adsorber. $\eta$ is the bulk porosity, $\eta_{\mathrm{P}}$ is the intraparticle porosity, $F_i$ is the amount of component $i$ added to the adsorber in the inlet stream, and $W_i$ is the corresponding amount removed in the outlet stream.

The differential material balance to the $i$th component of an $m$-component mixture in the adsorber yields

$$\eta\, \mathrm{d}c_i + (1-\eta)\eta_{\mathrm{P}}\, \mathrm{d}q_i = \mathrm{d}F_i - \mathrm{d}W_i, \tag{1}$$

where $c_i$ and $q_i$ are the concentrations in the bulk fluid and adsorbed phase, respectively. Since the fluid phase is assumed to be perfectly mixed

$$\mathrm{d}W_i = y_i\, \mathrm{d}W = c_i\, \mathrm{d}G, \tag{2}$$

where $y_i$ is the mole fraction of component $i$ in the fluid phase and $\mathrm{d}G$ is the differential volume of fluid (at the conditions prevailing in the adsorber) removed in the outlet stream, per unit volume of adsorber. Substitution of Eq. (2) into Eq. (1) gives

$$\eta\, \mathrm{d}c_i + (1-\eta)\eta_{\mathrm{P}}\, \mathrm{d}q_i = \mathrm{d}F_i - c_i\, \mathrm{d}G. \tag{3}$$

Integrating Eq. (3) from state $n-1$ to state $n$, the following material balance is obtained:

$$\eta\Delta c_i^{(n)} + (1-\eta)\eta_{\mathrm{P}}\Delta q_i^{(n)} = \Delta F_i^{(n)} - \bar{c}_i^{(n-1/2)}\Delta G^{(n)}, \tag{4}$$

where $\Delta\phi^{(n)} \equiv \phi^{(n)} - \phi^{(n-1)}$, the superscript denotes the state at which the evaluation takes place, and

$$\bar{c}_i^{(n-1/2)} = \frac{1}{\Delta G^{(n)}}\int_0^{\Delta G^{(n)}} c_i\, \mathrm{d}G \tag{5}$$

is the average concentration of component $i$ in the volume $\Delta G^{(n)}$ of fluid removed in the outlet stream.

If $\Delta G^{(n)}$ is small enough then a first-order implicit approximation for Eq. (5) holds,

$$\bar{c}_i^{(n-1/2)} = c_i^{(n)} + O\left[\Delta G^{(n)}\right], \tag{6}$$

and Eq. (4) can be approximated as

$$\begin{aligned}\left[\eta + \Delta G^{(n)}\right]c_i^{(n)} &+ (1-\eta)\eta_{\mathrm{P}}q_i^{(n)} \\ &= \eta c_i^{(n-1)} + (1-\eta)\eta_{\mathrm{P}}q_i^{(n-1)} + \Delta F_i^{(n)}.\end{aligned} \tag{7}$$

By repeatedly solving Eq. (7), the response of the adsorber to a given set of input parameters and operating conditions can be determined.

Since the inlet value $\Delta F_i^{(n)}$ is in most cases an input parameter, the terms on the r.h.s. of Eq. (7) are usually known quantities; we assume this to be the case here. To simplify the notation, the r.h.s. of Eq. (7) is condensed into a single parameter denoted by $w_i$ and the superscripts are dropped. Equation (7) becomes

$$(\eta + \Delta G)c_i + (1-\eta)\eta_{\mathrm{P}}q_i = w_i. \tag{8}$$

The $m$ material balances given by this equation are constrained by the conditions of thermodynamic

TABLE I Set of input parameters and output variables for each type of problem formulation

| *Type* | *Input parameters* | *Output variables* |
|---|---|---|
| I | $w_i$, $\Delta G$ | $P$, $c_i$, $q_i$ |
| II | $w_i$, $P$ | $\Delta G$, $c_i$, $q_i$ |

equilibrium for an isothermal adsorption system (equality of chemical potentials between the phases), and require a closure equation involving either $\Delta G$ or the pressure $P$ at the new state. Typically, the closure condition is simply assigning a value to one of these variables. Table I outlines the two distinct problem formulations that can arise, depending on the assigned variable. Provided that the correct specification variables are selected, Eq. (8) encompasses all possible operating modes of the adsorber. In this paper, it is shown that the problem formulated above can be solved by the GEMC method in the modified form presented next.

## SIMULATION METHOD

In the GEMC method [5–7] the two phases are simulated as two separate boxes, thereby avoiding problems with the direct simulation of the interface between the two phases. The system temperature $T$ is specified in advance and the number of molecules of each species $i$ in the adsorbed phase, $N_{i\mathrm{P}}$, and in the bulk, $N_{i\mathrm{B}}$, may vary according to the constraint $N_{i\mathrm{B}} + N_{i\mathrm{P}} = N_i$, where $N_i$ is fixed.

To develop a methodology for solving Eq. (8) using a Monte Carlo method, it is convenient to rewrite the equation in terms of $N_{i\mathrm{B}}$ and $N_{i\mathrm{P}}$. The resulting expression is

$$N_{i\mathrm{B}} + N_{i\mathrm{P}} = C_i \equiv \frac{N_{\mathrm{Av}} V_{\mathrm{P}}}{(1-\eta)\eta_{\mathrm{P}}} w_i, \tag{9}$$

where $N_{\mathrm{Av}}$ is avogadro's number and $V_{\mathrm{P}}$ is the volume of the box simulating the adsorbed phase. The value of $C_i$ is purposively expressed as a function of $V_{\mathrm{P}}$ instead of the volume $V_{\mathrm{B}}$ of the box simulating the bulk fluid. The reason for this is that $V_{\mathrm{P}}$ is always fixed, whereas, as we shall see below, $V_{\mathrm{B}}$ must be allowed to fluctuate during the course of the simulation when the pressure is an input parameter. Note, however, that since Eq. (9) is simply a restatement of Eq. (8) at molecular scale, $V_{\mathrm{B}}$ and $V_{\mathrm{P}}$ are constrained by the following condition:

$$\frac{V_{\mathrm{B}}}{\eta + \Delta G} = \frac{V_{\mathrm{P}}}{(1-\eta)\eta_{\mathrm{P}}}. \tag{10}$$

That is, the two simulation boxes must preserve the bulk to internal porosity ratio of the macroscopic system.

Since the GEMC method inherently conserves the total number of molecules of each species, Eq. (9) is automatically satisfied by every sampled configuration provided that each $C_i$ is an integer number. This feature of the Gibbs ensemble makes it the natural ensemble for solving Eq. (9). Although for a binary mixture it is possible to size $V_{\mathrm{B}}$ and $V_{\mathrm{P}}$ according to Eq. (10) so that each $C_i$ is an integer number, that is not the case for more complex mixtures. For the general case of an arbitrary multicomponent mixture, Eq. (9) is instead satisfied statistically by allowing the total number of molecules of each species to fluctuate around the target value $C_i$ so that the ensemble average gives

$$\langle N_i \rangle = C_i. \tag{11}$$

The procedure to generate trial configurations whose statistical average obeys Eq. (11) is discussed in "Acceptance Criterium for Particle Fluctuation Section".

Regardless of the type of problem (either type I or II) being solved, thermodynamic equilibrium between the two subsystems is achieved by allowing them to undergo configurational and particle transfer moves. For an attempted change of the internal configuration of one of the boxes (molecule displacement, rotation, or conformational change), the probability of acceptance is the same as for a conventional canonical simulation [19], i.e.

$$\min\{1, \exp(-\beta \Delta U)\}, \tag{12}$$

where $\beta = 1/k_{\mathrm{B}}T$, with $k_{\mathrm{B}}$ the Boltzmann's constant, and $\Delta U$ is the internal energy change resulting from the configurational move.

To satisfy equality of chemical potentials, transfers of particles between the two boxes are attempted. The probability of accepting a move in which a particle of type $i$ is transferred from the bulk fluid to the adsorbed phase is given by

$$\begin{aligned} &\mathrm{acc}(N_{i\mathrm{P}} \to N_{i\mathrm{P}} + 1; N_{i\mathrm{B}} \to N_{i\mathrm{B}} - 1) \\ &\quad = \min\left\{1, \frac{N_{i\mathrm{B}} V_{\mathrm{P}}}{(N_{i\mathrm{P}} + 1) V_{\mathrm{B}}} \exp(-\beta \Delta U)\right\}, \end{aligned} \tag{13}$$

where $\Delta U = \Delta U_{\mathrm{B}} + \Delta U_{\mathrm{P}}$ is the total internal energy change resulting from the particle transfer. Analogously, if a particle of type $i$ moves from the adsorption box to the bulk cell, the acceptance probability is

$$\begin{aligned} &\mathrm{acc}(N_{i\mathrm{P}} \to N_{i\mathrm{P}} - 1; N_{i\mathrm{B}} \to N_{i\mathrm{B}} + 1) \\ &\quad = \min\left\{1, \frac{N_{i\mathrm{P}} V_{\mathrm{B}}}{(N_{i\mathrm{B}} + 1) V_{\mathrm{P}}} \exp(-\beta \Delta U)\right\}. \end{aligned} \tag{14}$$

Equations (13) and (14) imply that sampling is performed by choosing a phase first, then a species, and finally selecting a molecule of that species for transfer to the other phase. If the sampling is done differently, the two equations must be modified accordingly.

For type I problems (see Table I) the sizes of the two simulation boxes are fixed and their volumes are related by Eq. (10). Since only ordinary MC moves and particle transfers are required to bring two isothermal boxes of fixed volume into equilibrium, the simulation scheme outlined above is sufficient for solving these problems. Note, however, that the pressure is not a direct output of the simulation. In practice this poses no problem, since $P$ can be related to the bulk density and composition through an equation of state. If the equation of state for the fluid is unknown, $P$ can be estimated during the simulation via calculation of the virial.

On the other hand, when the value of $P$ is imposed (type II problem), the volume $V_{\mathrm{B}}$ must be allowed to fluctuate so that on average the fluid contained within it is at the desired pressure. Once the ensemble average $\langle V_{\mathrm{B}}\rangle$ is determined, the value of $\Delta G$ follows from Eq. (10):

$$\Delta G = (1-\eta)\epsilon_{\mathrm{P}}\frac{\langle V_{\mathrm{B}}\rangle}{V_{\mathrm{P}}} - \eta. \tag{15}$$

Thus, the solution of a type II problem requires an additional type of move, which consists of randomly changing the volume of the bulk box. Such an attempted volume change, say from $V_{\mathrm{B}}$ to $V'_{\mathrm{B}}$, is accepted with probability

$$\begin{aligned}\mathrm{acc}(V_{\mathrm{B}} \to V'_{\mathrm{B}}) = \min\langle 1, \exp\{-\beta[\Delta U_{\mathrm{B}} + P(V'_{\mathrm{B}} - V_{\mathrm{B}})\\ - \beta^{-1}N_{\mathrm{B}}\ln(V'_{\mathrm{B}}/V_{\mathrm{B}})]\}\rangle,\end{aligned} \tag{16}$$

where $\Delta U_{\mathrm{B}}$ is the internal energy change resulting from the volume move. Overall, this acceptance criterium is identical to that for volume changes in the isothermal–isobaric ensemble, and is a particular case of the acceptance rule for the constant-pressure Gibbs ensemble method [6]. When the rules given here for type II problems are applied to a single adsorbate, they become identical to those of McGrother and Gubbins [20] in their simulation technique for the study of single-component adsorption.

## Short-cut Method

We assume hereafter that an analytical equation of state for the fluid phase is known. This assumption is usually valid for adsorption applications from the gas phase, which are our main application target. It is shown next that if an analytical equation of state for the fluid phase is known, the simulation procedure can be considerably simplified. The resulting method can be viewed as a hybrid of the conventional GCMC and GEMC techniques.

Let us first assume that the pressure in the adsorber is sufficiently low for the molecules to behave like an ideal gas and, therefore, to not interact when they are in volume $V_{\mathrm{B}}$. If one of the $N_{i\mathrm{B}}$ particles in volume $V_{\mathrm{B}}$ is transferred to volume $V_{\mathrm{P}}$, the total potential energy $U$ changes by $\Delta U_{\mathrm{P}}(\mathbf{s}^{N_{i\mathrm{P}}+1}) = U_{\mathrm{P}}(\mathbf{s}^{N_{i\mathrm{P}}+1}) - U_{\mathrm{P}}(\mathbf{s}^{N_{i\mathrm{P}}})$, where $\mathbf{s}^{N_{i\mathrm{P}}}$ represents the coordinates of the $N_{i\mathrm{P}}$ particles in volume $V_{\mathrm{P}}$. Likewise, if a particle of type $i$ is moved to volume $V_{\mathrm{B}}$, the total potential energy change resulting from the move is $\Delta U_{\mathrm{P}}(\mathbf{s}^{N_{i\mathrm{P}}-1}) = U_{\mathrm{P}}(\mathbf{s}^{N_{i\mathrm{P}}-1}) - U_{\mathrm{P}}(\mathbf{s}^{N_{i\mathrm{P}}})$. Thus, for an ideal gas the probabilities of accepting a trial particle transfer are identical to those given by Eqs. (13) and (14), except that $\Delta U_{\mathrm{B}} = 0$. This simplification reduces both the complexity of the code and the CPU time, since the only data for the bulk box that must be updated during the course of the simulation is the integer array $\mathbf{N}_{\mathrm{B}} \equiv [N_{1\mathrm{B}}, \ldots, N_{m\mathrm{B}}]$ holding the number of molecules of each species in volume $V_{\mathrm{B}}$. As we shall see later, the use of an equation of state to determine the configuration of box $V_{\mathrm{B}}$ has other fortunate implications.

For an ideal gas the chemical potential, $\mu$, is related to the number density, $\rho_{N_{\mathrm{B}}} = N_{\mathrm{B}}/V_{\mathrm{B}}$, by $\mu = \beta^{-1}\ln(\Lambda^3\rho_{N_{\mathrm{B}}})$, where $\Lambda$ is the thermal de Broglie wavelength. Therefore, for an ideal gas mixture the acceptance probabilities given by Eqs. (13) and (14) can be rewritten as

$$\begin{aligned}&\mathrm{acc}(N_{i\mathrm{P}} \to N_{i\mathrm{P}}+1; N_{i\mathrm{B}} \to N_{i\mathrm{B}}-1)\\ &= \min\left\langle 1, \frac{V_{\mathrm{P}}}{\Lambda_i^3(N_{i\mathrm{P}}+1)}\exp\left\{-\beta\left[\Delta U(\mathbf{s}^{N_{i\mathrm{P}}+1}) - \mu_{N_{i\mathrm{B}}}\right]\right\}\right\rangle,\end{aligned} \tag{17}$$

$$\begin{aligned}&\mathrm{acc}(N_{i\mathrm{P}} \to N_{i\mathrm{P}}-1; N_{i\mathrm{B}} \to N_{i\mathrm{B}}+1)\\ &= \min\left\langle 1, \frac{\Lambda_i^3 N_{i\mathrm{P}}}{V_{\mathrm{P}}}\exp\left\{-\beta\left[\Delta U(\mathbf{s}^{N_{i\mathrm{P}}-1}) + \mu_{N_{i\mathrm{B}}+1}\right]\right\}\right\rangle.\end{aligned} \tag{18}$$

Note that in these acceptance rules the bulk system is referenced solely through the chemical potential,

$$\mu_{N_{i\mathrm{B}}+k} \equiv \mu(\rho_{N_{i\mathrm{B}}+k}, T), \quad \rho_{N_{i\mathrm{B}}+k} = (N_{i\mathrm{B}}+k)/V_{\mathrm{B}}, \tag{19}$$

and that any explicit reference to $V_{\mathrm{B}}$ has disappeared.

Although it is perfectly permissible to work with chemical potentials, adsorption experiments are usually reported as a function of the pressure and composition of the bulk fluid. As discussed above, if the density of the gas is sufficiently low, such that it behaves like an ideal gas, the term $\exp(\beta\mu_{N_{i\mathrm{B}}+k})/\Lambda_i^3$ in Eqs. (17) and (18) can be replaced by $\beta P(\rho_{N_{i\mathrm{B}}+k}, T) = \rho_{N_{i\mathrm{B}}+k}$, where $P(\rho_{N_{i\mathrm{B}}+k}, T)$ is the pressure exerted by an ideal gas with number density $\rho_{N_{i\mathrm{B}}+k}$ at temperature $T$. If the pressure is too high for

```
Full method                                                      Shortcut method
                                                                    (changes)
Select a species $i$ at random
Generate a random number $\xi$, $0 \le \xi < 1$
IF $N_{iB} + N_{iP} = int(C_i)$ THEN
  IF $\xi < \delta_i$ THEN
    Create a new molecule of type $i$ in volume $V_B$        $N_{iB} := N_{iB} + 1$
  END IF
ELSE IF $\xi > \delta_i$ THEN
  IF $N_{iB} > 0$ THEN
    Destroy a molecule of type $i$ in volume $V_B$           $N_{iB} := N_{iB} - 1$
  ELSE
    Destroy a molecule of type $i$ in volume $V_P$
  END IF
END IF
```

FIGURE 2 Algorithm of trial move to adjust the total number of molecules of type *i* according to the probability distribution given by Eq. (22). The left-hand column lists the implementation for the case where molecules are explicitly modeled in both simulation boxes (full method); the right-hand column lists the simplifications for the short-cut method in which the configuration of the bulk simulation box is determined by an equation of state. In the latter case, the procedure for inserting (removing) a gaseous molecule in the bulk box is reduced to a mere increment (decrement) of the counter of the total number of molecules of that type (see "Acceptance Criterium for Particle Fluctuation Section").

the ideal gas law to hold, $P(\rho_{N_{iB}+k}, T)$ must be replaced by the fugacity $\hat{f}_i(\mathbf{N}_B, k, T)$ of species $i$ at temperature $T$ in the gas mixture of number density $\rho_{N_B+k}$ and mole-fraction composition

$$y_1 = \frac{N_{1B}}{N_B + k}, \ldots, y_i = \frac{N_{iB} + k}{N_B + k}, \ldots, y_m = \frac{N_{mB}}{N_B + k}. \quad (20)$$

The method of employing $\mathbf{N}_B$ and the equation of state to compute $\hat{f}_i$ depends on the type of problem being solved. If $\Delta G$ is an input parameter (type I problem), $V_B$ is fixed during the course of the simulation and the gas mixture is further specified by its number density $\rho_{N_B+k} = (N_B + k)/V_B$. If, on the other hand, the pressure is fixed (type II problem), the value of $P$ defines the state of the mixture.

### Acceptance Criterium for Particle Fluctuation

In order to complete the simulation procedure it is necessary to generate trial configurations whose statistical average obeys Eq. (11). Let us consider how to do this. First, note that the maximum number of molecules of species $i$ that may exist in the simulation system without exceeding the material balance imposed by Eq. (9) is obtained by truncating $C_i$ to an integer number, which we denote by $int(C_i)$. The remainder $\delta_i$ $(0 \le \delta_i < 1)$, which must be added to $int(C_i)$ to get $C_i$, is

$$\delta_i = C_i - int(C_i). \quad (21)$$

To get the best statistics $N_i = N_{iB} + N_{iP}$ must fluctuate with the smallest amplitude around the target value $C_i$, which is the case when $N_i$ can only have the integer values $int(C_i)$ or $int(C_i) + 1$. It is straightforward to derive that for Eq. (11) to hold, the probability density of finding the system in one of the two configurations must be

$$\begin{aligned} \mathcal{N}\{N_i \rightarrow int(C_i)\} &\propto 1 - \delta_i, \\ \mathcal{N}\{N_i \rightarrow int(C_i) + 1\} &\propto \delta_i. \end{aligned} \quad (22)$$

In order to sample this probability distribution, a new type of trial move must be performed which consists of an attempt to change the system to a configuration with $int(C_i)$ or $int(C_i) + 1$ particles. The box for insertion or removal of the molecule must be selected with a fixed probability, which may be different for each box. In fact, we advocate that insertions and removals take place in the bulk box, except for the infrequent case that the number of particles of the selected species in volume $V_B$ becomes zero after a successful transfer to the adsorption box. This choice is most suited to adsorption from the gas phase where, in general, the bulk phase is much less dense than the adsorbed phase and, therefore, more permeable to particle insertions. The algorithm implementing this trial move is listed in the left-hand column of Fig. 2. Note that the algorithm is heuristic, since the probability density given by Eq. (22) does not depend on the molecular configuration of the system. That is, it is not specified how to actually choose the molecule if one is to be destroyed nor how to select the insertion position if one is being created. However, these troublesome details disappear altogether when the short-cut version of our method is employed, because, as described above, the potential energy of volume $V_B$ is then determined solely by the equation of state. In this case the procedure for inserting or removing a gaseous molecule of type $i$ is greatly simplified, it is just the update of the value of counter $N_{iB}$. This is highlighted in the right-hand column of Fig. 2.

## RESULTS AND DISCUSSION

For illustration purposes the pore space of the adsorbent is assumed to consist of slit-shaped pores of width $h_P = 15$ Å, with parameters chosen to model activated carbon. This is the simplest idealized representation of a porous carbon that is suitable for molecular simulation work [21]. It has been used extensively to study adsorption in porous carbons [22–24]. The porosity values are fixed at $\eta = 0.45$ and $\eta_P = 0.6$; they represent typical values for a packed bed of granular activated carbon.

The adsorbates considered in this study are hydrogen, methane and ethane. We adopted a united-atom description based on the Lennard–Jones 12-6 potential to describe the nonbonded interaction energy. Methane and ethane were modeled using the TraPPE [25] force field, which was developed from calculations for the vapour–liquid coexistence curve of the bulk fluids and reproduces accurately the experimental liquid densities and critical parameters. The LJ parameters for $H_2$ were taken from Turner *et al.* [26]. Unlike interactions were computed using standard Lorentz–Berthelot combing rules [19]. The potential cut-off was set at 14 Å, with no long-range corrections applied. The gas-phase fugacities $\hat{f}_i$ were computed from the virial equation, truncated at the second coefficient. Pure-component and mixture interaction coefficients were estimated using the formulas given by Reid *et al.* [27].

The interactions with the carbon walls were accounted for using the structureless 10-4-3 potential of Steele [28]. The solid–fluid potential $U_s(z_i)$ experienced by a molecule of type $i$ at a position $z_i$ in the slit pore is the sum of the interactions with graphite planes beneath and above:

$$U_s(z_i) = u_s(z_i) + u_s(h_P - z_i), \tag{23}$$

where

$$u_s(z_i) = 2\pi\rho_s\epsilon_{iC}\sigma_{iC}^2\Delta_s \times \left[\frac{2}{5}\left(\frac{\sigma_{iC}}{z_i}\right)^{10} - \left(\frac{\sigma_{iC}}{z_i}\right)^4 - \frac{\sigma_{iC}^4}{3\Delta_s(z_i+0.61\Delta_s)}\right]. \tag{24}$$

Here, $\rho_s = 0.114\,\text{Å}^{-3}$ is the density of the carbon, $\Delta_s = 3.35\,\text{Å}$ is the spacing of the graphite planes, and $\epsilon_{iC}$ and $\sigma_{iC}$ are the LJ parameters for the interaction between carbon atoms and pseudo-atom $i$.

Each simulation run was equilibrated for $10^4$ Monte Carlo cycles, where each cycle consists of $N$ attempts to change the internal configuration of volume $V_P$ (equally partitioned between translations and conformational changes) and $N/3$ attempts to transfer a molecule between the two boxes. Each molecule transfer attempt was followed by a trial move to adjust the total number of molecules of that type according to the probability distribution given by Eq. (22). The production periods consisted of $3\times10^4$ Monte Carlo cycles. The maximum displacements for translations and rotations in the pore box were adjusted during the equilibration phase to give a 50% acceptance rate. Standard deviations of the ensemble averages were computed by breaking the production runs into five blocks.

## Testing and Validation

In order to validate our method, and in particular the applicability of its short-cut version to simulate adsorption from the gas phase, a series of preliminary simulations has been performed. The simplest test that can be done is to generate the pure-component adsorption isotherm for a given adsorbate by charging the adsorber with various amounts of pure gas to equilibrate the system at different pressures. Each run is equivalent to solving Eq. (8) as a type I problem with $\Delta G = 0$ and $w = \Delta F$, where $\Delta F$ is the charge amount. Prior to each run the size of the simulation boxes was adjusted to give an average number of gaseous particles $\langle N_B\rangle = 5$. This number was purposively chosen small, since any discrepancies in the results generated by an incorrect sampling scheme are better detected for small system sizes. The adsorption isotherms for the three adsorbates as obtained using our short-cut method were compared with those given by the standard GCMC technique. The results obtained (not plotted here to save space) were in excellent agreement with the GCMC results, which attests to the correctness of our sampling scheme. Overall, these test runs demonstrate that our scheme correctly samples phase space and that for the adsorbates under study the concentration of the adsorbed phase can be accurately determined using a very modest average number of molecules in the bulk box. This is important, since there are instances of many practical adsorptive separation processes when one or more components are present in diluted concentration.

In order to further validate our method for multicomponent adsorption, a second series of tests has been performed. These were divided into three sets, each consisting on the pressurization of the adsorber with four ternary mixtures of different compositions. In the first set of runs, which is referred to as set G-NVT, Eq. (8) was solved with closure condition $\Delta G = 0$, $w_i = y_i^{\text{in}}\Delta F$, where $y_i^{\text{in}}$ is the mole fraction of the $i$th component in the inlet gas, and the equilibrium pressure as one output of the simulation. There runs are similar to the single-component tests reported above. Then, a second set of runs (G-NPT) was performed using the same feed mixtures and the pressure fixed at the values obtained from the G-NVT runs. Note that these are type II problems in which $\langle V_B\rangle$ is an output of the simulation. Finally, a third set of runs (GCMC) was carried out to check the accuracy of the previous results. These runs consisted of standard multi-component GCMC simulations with mixture fugacities calculated from the virial equation of state using the pressures and gas-phase compositions obtained in the G-NVT runs.

The results obtained are listed in Table II. The three sets of simulations give the same results to within statistical uncertainty, which again attests to the viability of the proposed method. The total number of molecules employed in the G-NVT and G-NPT runs is listed in the 8th column of Table II. They were intentionally set to noninteger values to test the efficiency of the sampling method given by

TABLE II Results of validation tests (the subscripts indicate the estimated error in the last digit of the value)

| $\Delta F$ (*mol/m$^3$*) | $y_1^{in}$ (%) | $y_2^{in}$ (%) | $y_3^{in}$ (%) | *Type* | $L_P$ (*Å*) | $L_B$ (*Å*) | *N* | $\langle P\rangle$ (*bar*) | $\langle q\rangle$ (*mol/m$^3$*) | $\langle N_P\rangle$ | $\langle x_1\rangle$ (%) | $\langle x_2\rangle$ (%) | $\langle x_3\rangle$ (%) | $\langle c\rangle$ (*mol/m$^3$*) | $\langle N_B\rangle$ | $\langle y_1\rangle$ (%) | $\langle y_2\rangle$ (%) | $\langle y_3\rangle$ (%) |
|---|---|---|---|---|---|---|---|---|---|---|---|---|---|---|---|---|---|---|
| 70 | 30 | 50 | 20 | G-NVT | 510.8 | 174.8 | 500.01 | $0.5131_8$ | $183.90_5$ | $433.5_1$ | $31.23_4$ | $56.74_2$ | $12.03_5$ | $20.70_3$ | $66.5_1$ | $21.9_3$ | $6.11_4$ | $72.0_3$ |
| | | | | G-NPT | | | | | $183.87_8$ | $433.4_2$ | $31.21_2$ | $56.75_2$ | $12.04_3$ | $20.70_0$ | $66.6_2$ | $21.9_1$ | $6.14_6$ | $72.0_1$ |
| | | | | GCMC* | | | | | $184.4_8$ | $434.7_{19}$ | $31.2_3$ | $56.8_3$ | $12.05_5$ | | | | | |
| 270 | 40 | 40 | 20 | G-NVT | 260.2 | 111.5 | 500.50 | $2.119_9$ | $701.6_5$ | $429.2_3$ | $42.09_4$ | $45.89_3$ | $12.02_5$ | $85.5_4$ | $71.3_3$ | $27.3_3$ | $4.57_5$ | $68.1_2$ |
| | | | | G-NPT | | | | | $700.9_8$ | $428.7_5$ | $42.05_4$ | $45.94_5$ | $12.01_6$ | $85.5_0$ | $71.8_5$ | $27.5_2$ | $4.61_6$ | $67.9_2$ |
| | | | | GCMC* | | | | | $704.6_{40}$ | $431.0_{24}$ | $41.7_3$ | $46.4_3$ | $11.9_1$ | | | | | |
| 1500 | 80 | 10 | 10 | G-NVT | 110.4 | 62.9 | 500.10 | $11.66_4$ | $3900_2$ | $429.2_2$ | $83.10_5$ | $11.46_1$ | $5.45_5$ | $473_1$ | $70.9_2$ | $61.1_3$ | $1.21_3$ | $37.7_3$ |
| | | | | G-NPT | | | | | $3885_8$ | $427.5_9$ | $83.06_5$ | $11.50_2$ | $5.44_7$ | $472.8_0$ | $72.6_9$ | $61.6_2$ | $1.21_3$ | $37.2_2$ |
| | | | | GCMC* | | | | | $3890_{13}$ | $428.0_{14}$ | $83.0_1$ | $11.5_1$ | $5.50_8$ | | | | | |
| 3515 | 8 | 90 | 2 | G-NVT | 72.1 | 47.4 | 500.50 | $10.63_9$ | $10053_6$ | $472.4_3$ | $6.81_4$ | $92.65_5$ | $0.54_1$ | $439_4$ | $28.1_3$ | $27.9_6$ | $45.2_6$ | $26.9_3$ |
| | | | | G-NPT | | | | | $10032_{24}$ | $471.4_{11}$ | $6.74_9$ | $92.7_1$ | $0.55_2$ | $438.7_3$ | $29.1_{11}$ | $28.2_9$ | $45.1_8$ | $26.7_8$ |
| | | | | GCMC* | | | | | $10012_{32}$ | $470.5_{15}$ | $6.7_3$ | $92.7_3$ | $0.55_1$ | | | | | |

* Mixture fugacities calculated from the virial equation of state using pressure and gas-phase composition data from the corresponding G-NVT run.

Eq. (22). As is easily verified, there is very good agreement between $\langle N_B\rangle + \langle N_P\rangle$ and the imposed $N$ value for every run.

## Application Example

To illustrate the full potential use of the simulation technique described in this work, we apply it to generate the response of the adsorber under typical operating conditions of a batch adsorption process. The molar composition of the feed stream is 20% $H_2$, 30% $CH_4$ and 50% $C_2H_6$. The operation procedure consists of the following steps: (I) charge from vacuum up to $P = 10\,\text{bar}$, (II) constant-pressure feed, and (III) discharge down to $P = 1.25\,\text{bar}$. This example encompasses the major steps of every cyclic batch adsorption process for gas separation, in which regeneration of the bed is accomplished by reducing the pressure at essentially constant temperature, as is the case in pressure swing adsorption [29]. The input parameters and output variables for each phase of the process are listed in Table III.

Figure 3 shows the simulated pressure profile plotted as a function of either the amount of feed or product, depending on the particular step of the process. The corresponding density profile of the adsorbed phase is given in Fig. 4. As the adsorber is pressurized with feed, the adsorbed phase is enriched in methane and ethane, leaving most of the hydrogen in the gas phase. This is shown in Fig. 5, where we plot the simulated profiles of mole fraction in gas phase. For the thermodynamic conditions of this study, hydrogen can be considered as a nonadsorbing carrier. The pressure builds up linearly because the partial pressure of ethane, which is the only component whose adsorption isotherm is nonlinear, is kept in the Henry's law region. Consequently, $q = \sum q_i$ also varies linearly with $F$.

When the pressure in the adsorber attains the charge value, the outlet port is opened and product is removed at a variable rate in order to keep the pressure constant. Notice that although the adsorber is operated at constant pressure, there is significant accumulation of material in the adsorber, as shown by the curve $q(F^{\text{II}})$ in Fig. 4. This is because ethane is being heavily concentrated in the adsorbed phase. During the high-pressure adsorption step,

TABLE III Input parameters and output variables employed in each phase of the simulated operation of the adsorber

| *Phase* | *# steps* | *Input parameters* | | *Output variables* |
|---|---|---|---|---|
| I | 10 | $\Delta F^{(n)} = 126.5\,\text{mol/m}^3$ | $\Delta G^{(n)} = 0$ | $P^{(n)}$ |
| II | 36 | $^*\Delta F^{(n)} = c^{(n-1)}$ | $P^{(n)} = 10\,\text{bar}$ | $\Delta G^{(n)}$ |
| III | 21 | $\Delta F^{(n)} = 0$ | $^\dagger\Delta G^{(n)} = 100/c^{(n-1)}$ | $P^{(n)}$ |

$c = \sum c_i$. *Nearly equivalent to setting $\Delta F^{(n)} = 400\,\text{mol/m}^3$. †Nearly equivalent to setting $\Delta W^{(n)} = 90\,\text{mol/m}^3$.

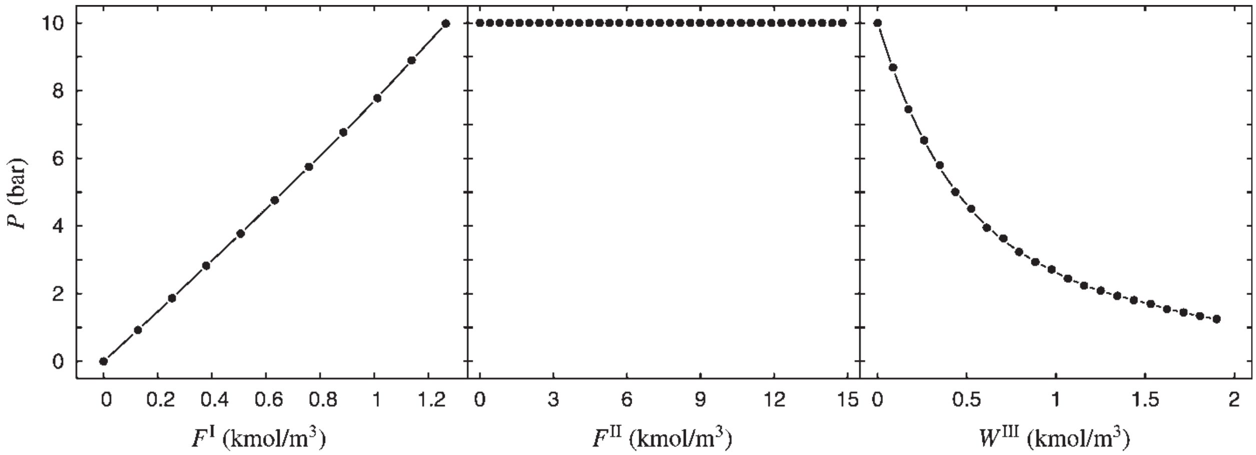

FIGURE 3 Simulated pressure profile in the adsorber plotted as a function of either the amount of feed *F* or product *W*, as applicable to each step of the process. The operating procedure consists of the following sequence of steps: (I) charge, (II) constant-pressure feed, and (III) discharge. The line is a smooth interpolation of the simulation data (symbols) and is included as a guide to the eye in the regions of lower data density. Note also that each step has been allotted the same space in order to make the plot more readable; in reality, step II is considerably longer than the other two steps.

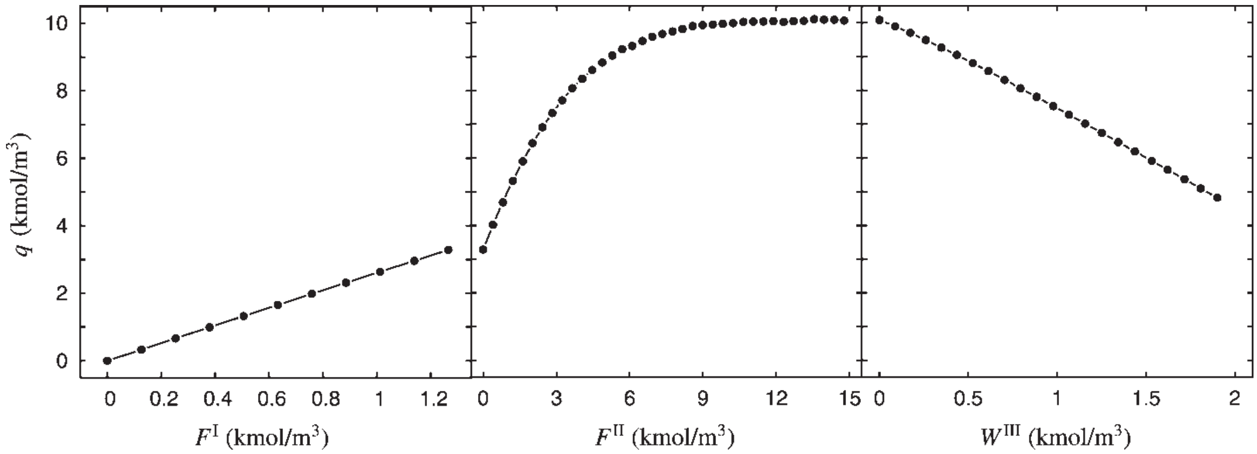

FIGURE 4 Simulated profile of total concentration in adsorbed phase during operation of the adsorber: (I) charge, (II) constant-pressure feed, (III) discharge. Additional comments are provided in the caption of Fig. 1.

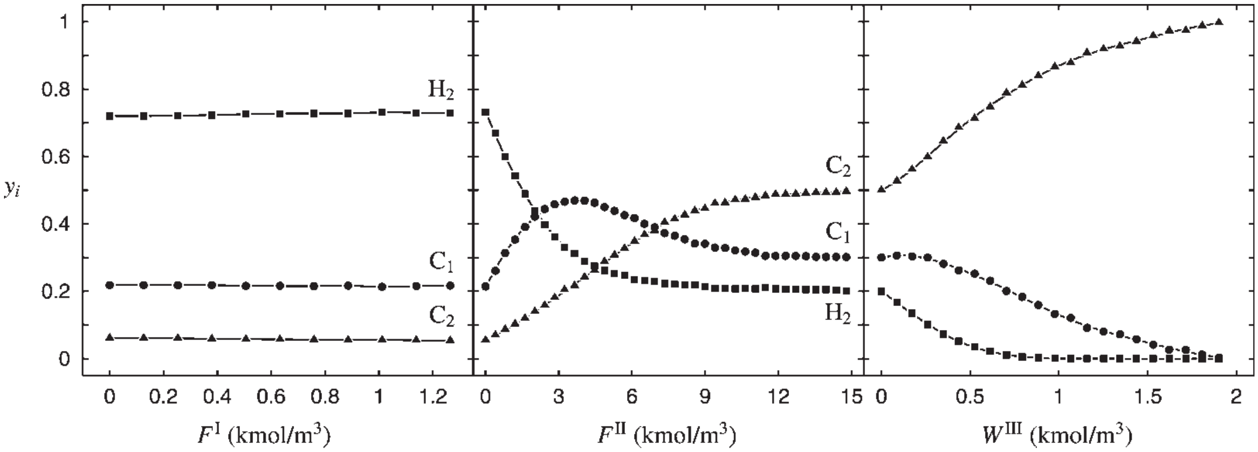

FIGURE 5 Simulated profiles of mole fraction in gas phase during operation of the adsorber: (I) charge, (II) constant-pressure feed, (III) discharge. (•) $CH_4$, (▲) $C_2H_6$, (■) $H_2$. See the caption of Fig. 1 for additional comments.

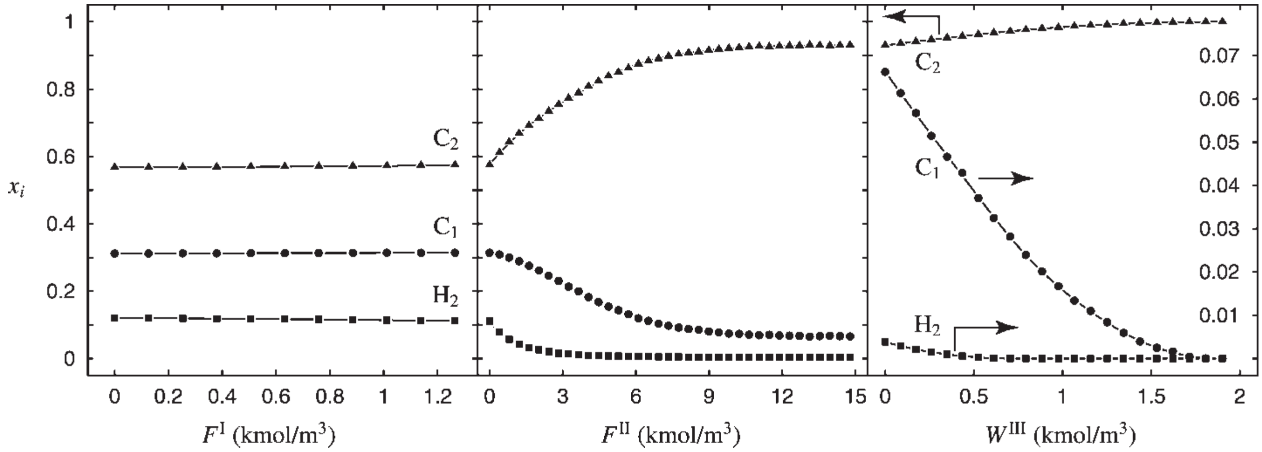

FIGURE 6 Simulated profiles of mole fraction in adsorbed phase during operation of the adsorber: (I) charge, (II) constant-pressure feed, (III) discharge. (•) $CH_4$, (▲) $C_2H_6$, (■) $H_2$. Additional comments are provided in the caption of Fig. 1.

the intermediate gaseous concentration of methane exceeds its concentration in the feed stream while that of hydrogen, which increased considerably during charge, now decreases steadily to its value in the feed (Fig. 5). The effect is due to the stronger affinity of the adsorbent for ethane, which progressively displaces methane from the adsorbed phase, thereby enriching the gas phase with this component. This is a common feature of multicomponent adsorption systems and is sometimes referred to as roll-up [30]. If the adsorption step is prolonged sufficiently, as is the case here, the composition of the adsorbed phase will equilibrate with that of the feed stream. From this point onward, the adsorber is saturated since there is no more accumulation of material within it and the composition of the product stream is equal to that of the feed.

During discharge, the adsorber is depressurized to give a product which is essentially pure ethane with some traces of methane. As opposed to what is seen during pressurization, the pressure profile is highly nonlinear during discharge. $P$ drops quicker during the initial stage of discharge than when the adsorber is more depleted. The reason for this nonlinear behavior is the strong affinity of the microporous carbon for ethane, which is by far the predominant species in the adsorber during discharge (Fig. 6). Since the product is mainly taken from the adsorbed phase, $q$ decreases almost linearly with $W$ (cf. Fig. 4) and, therefore, the shape of the curve $P(W^{III})$ is a direct consequence of the curvature of the adsorption isotherm for ethane.

## CONCLUSIONS

The theoretical approach presented here is an attempt to develop an *ab-initio* or *first-principles* computational methodology to predict the macroscopic behavior of an adsorption process from knowledge of the intermolecular forces and structural characteristics of the adsorbent. The method is not restricted to adsorption processes, and is equally applicable, for example, to vapor–liquid equilibrium if the adsorption box is replaced by a box simulating the bulk liquid. In this case the procedure would simulate the behavior of a flash unit with an imposed operating temperature.

For simplicity, the application example presented in this work has been restricted to small molecules and to a simple pore structure. The usefulness of the proposed molecular simulation technique certainly increases with the complexity of the solid–fluid adsorption system under study. When the adsorbed phase is very dense and for situations where complex molecules are involved, standard particle insertion and transfer moves become impractical due to steric overlap. To enhance the sampling of chain molecules at high density in the proposed method, configurational-biased techniques [31–33] can be easily applied in which a molecule is inserted segment by segment such that configurations with favorable energies are preferred. The bias introduced in finding an improved conformation for the molecule is then accounted for by changing the acceptance criterium.

We are currently extending the methodology to handle the more general case of a nonisothermal adsorption system. The use of molecular simulation techniques, such as the one presented here, could grow in importance, gradually supplanting many empirical constitutive models that are used in process-scale calculations today.

### *References*

[1] Nicholson, D. and Parsonage, N.G. (1982) *Computer Simulation and the Statistical Mechanics of Adsorption* (Academic Press, London).

[2] de Pablo, J.J. and Escobedo, F.A. (2002) "Molecular simulations in chemical engineering: present and future", *AIChE J.* **48**, 2716.

[3] Adams, D.J. (1975) "Grand canonical ensemble Monte Carlo for a Lennard–Jones fluid", *Mol. Phys.* **29**, 307.

[4] van Megen, W. and Snook, I.K. (1982) "Physical adsorption of gases at high pressure. I. The critical region", *Mol. Phys.* **45**, 629.

[5] Panagiotopoulos, A.Z. (1987) "Direct determination of phase coexistence properties of fluids by Monte Carlo simulation in a new ensemble", *Mol. Phys.* **61**, 813.

[6] Panagiotopoulos, A.Z., Quirke, N., Stapleton, M. and Tildesley, D.J. (1988) "Phase equilibria by simulations in the Gibbs ensemble: alternative derivation, generalization and application to mixtures and membrane equilibria", *Mol. Phys.* **63**, 527.

[7] Smit, B. and de Smedt, P.H. (1989) "Computer simulations in the Gibbs ensemble", *Mol. Phys.* **68**, 931.

[8] Panagiotopoulos, A.Z. (1987) "Adsorption and capillary condensation of fluids in cylindrical pores by Monte Carlo simulation in the Gibbs ensemble", *Mol. Phys.* **62**, 701.

[9] Jiang, S. and Gubbins, K.E. (1995) "Vapor–liquid equilibria in two-dimensional Lennard-Jones fluids: unperturbed and substrate-mediated films", *Mol. Phys.* **86**, 599.

[10] Gozdz, W.T., Gubbins, K.E. and Panagiotopoulos, A.Z. (1995) *Mol. Phys.* **84**, 825.

[11] Kofke, D.A. (1993) "Direct evaluation of phase coexistence by molecular simulation via integration along the saturation line", *J. Chem. Phys.* **98**, 4149.

[12] Kofke, D.A. (1999) "Semigrand canonical Monte Carlo simulations: integration along coexistence lines", *Adv. Chem. Phys.* **105**, 405.

[13] Kofke, D.A. and Glandt, E.D. (1988) "Monte Carlo simulation of multicomponent equilibria in a semigrand canonical ensemble", *Mol. Phys.* **64**, 1105.

[14] Mehta, M. and Kofke, D.A. (1994) "Coexistence diagrams of mixtures by molecular simulation", *Chem. Eng. Sci.* **49**, 2633.

[15] Mehta, M. and Kofke, D.A. (1995) "Molecular simulation in a pseudo grand-canonical ensemble", *Mol. Phys.* **86**, 139.

[16] Escobedo, F.A. (1998) "Novel pseudoensembles for simulation of multicomponent phase equilibria", *J. Chem. Phys.* **108**, 8761.

[17] Escobedo, F.A. (1999) "Tracing coexistence lines in multicomponent fluid mixtures by molecular simulation", *J. Chem. Phys.* **110**, 11999.

[18] Escobedo, F.A. (2000) "Molecular and macroscopic modeling of phase separation", *AIChE J.* **46**, 2086.

[19] Frenkel, D. and Smit, B. (1996) *Understanding Molecular Simulation* (Academic Press, New York).

[20] McGrother, S.C. and Gubbins, K.E. (1999) "Constant pressure Gibbs ensemble Monte Carlo simulations of adsorption into narrow pores", *Mol. Phys.* **97**, 955.

[21] Gelb, L.V., Gubbins, K.E., Radhakrishnan, R. and Sliwinska-Bartkowiak, M. (1999) "Phase separation in confined system", *Rep. Prog. Phys.* **62**, 1573.

[22] Tan, Z. and Gubbins, K.E. (1990) "Adsorption in carbon micropores at supercritical temperatures", *J. Phys. Chem.* **94**, 6061.

[23] Matranga, K.R., Myers, A.L. and Glandt, E.D. (1991) "Storage of natural gas by adsorption on activated carbon", *Chem. Eng. Sci.* **47**, 1569.

[24] Cracknell, R.F., Gordon, P. and Gubbins, K.E. (1993) "Influence of pore geometry on the design of microporous materials for methane storage", *J. Phys. Chem.* **97**, 494.

[25] Martin, M.G. and Siepmann, J.I. (1998) "Transferable potentials for phase equilibria. 1. United-atom description of n-alkanes", *J. Phys. Chem. B* **102**, 2569.

[26] Turner, C.H., Pikunic, J. and Gubbins, K.E. (2001) "Influence of chemical and physical surface heterogeneity on chemical reaction equilibria in carbon micropores", *Mol. Phys.* **99**, 1991.

[27] Reid, R.C., Prausnitz, J.M. and Polling, B.E. (1988) *The Properties of Gases & Liquids*, 4th Ed. (McGraw-Hill, Singapore).

[28] Steele, W.A. (1974) *The Interaction of Gases with Solid Surfaces* (Pergamon, Oxford).

[29] Yang, R.T. (1997) *Gas Separation by Adsorption Processes* (Imperial College Press, London).

[30] Ruthven, D.M. (1984) *Principles of Adsorption & Adsorption Processes* (John Wiley, New York).

[31] Snurr, R.Q., Bell, A.T. and Theodorou, D.N. (1993) "Prediction of adsorption of aromatic hydrocarbons in silicalite from grand canonical Monte Carlo simulations with biased insertions", *J. Phys. Chem.* **97**, 13742.

[32] Smit, B. (1995) "Grand canonical Monte Carlo simulations of chain molecules: adsorption isotherms of alkanes in zeolites", *Mol. Phys.* **85**, 153.

[33] Macedonia, M.D. and Maggin, E.J. (1999) "A biased grand canonical Monte Carlo method for simulating adsorption using all-atom and branched united atom models", *Mol. Phys.* **96**, 1375.